Tragacanth Gum as Green Binder for Sustainable Water-Processable Electrochemical Capacitor

Alberto Scalia[+],[a] Pietro Zaccagnini[+],[a, b] Marco Armandi,[a] Giulio Latini,[a, b] Daniele Versaci,[a] Vittorino Lanzio,[a] Alberto Varzi,*[c, d] Stefano Passerini,[c, d] and Andrea Lamberti*[a, b]

Enabling green fabrication processes for energy storage devices is becoming a key aspect in order to achieve a sustainable fabrication cycle. Here, the focus was on the exploitation of the tragacanth gum, an exudated gum like arabic and karaya gums, as green binder for the preparation of carbon-based materials for electrochemical capacitors. The electrochemical performance of tragacanth (TRGC)-based electrodes was thoroughly investigated and compared with another water-soluble binder largely used in this field, sodium-carboxymethyl cellulose (CMC). Apart from the higher sustainability both in production and processing, TRGC exhibited a lower impact on the obstruction of pores in the final active material film with respect to CMC, allowing for more available surface area. This directly impacted the electrochemical performance, resulting in a higher specific capacitance and better rate capability. Moreover, the TRGC-based supercapacitor showed a superior thermal stability compared with CMC, with a capacity retention of about 80% after 10000 cycles at 70 °C.

Introduction

Electrochemical double layer capacitors (EDLCs) are receiving increasing interest in the scientific and industrial community due to their exceptional power density and long cycle life.[1] Such features have enabled a series of applications such as in hybrid vehicles, voltage stabilizers, power grid buffers, and so on.[2] Recently, in order to widen their application range, a considerable number of works have been published on electrolytes for high-voltage EDLCs, trying to narrow the gap with lithium-ion batteries (LIBs) regarding energy density.[3] Such effort is justified by the outstanding and incomparable number of cycles (up to 10^6) EDLCs can sustain with respect to the less durable LIB technology.[4] In fact, this feature makes them particularly interesting to be exploited in locations difficult to be reached, for applications requiring long life and no maintenance, such as intermittent renewable energy storage, or self-rechargeable portable power systems based on integrated energy harvesting and storage devices.[5]

Overall, for both EDLCs and LIBs research is trying to find green routes for their fabrication. In particular, a transition towards aqueous electrode processing, green electrolytes, active materials derived from biomaterials, and bio-derived polymers as binders is occurring, leading to lower costs and environmental impact.[6] These effects are not only due to the obvious cost-effectiveness of water as a solvent but, above all, to consideration of the investments and procedures that are necessary in the production plants in order to guarantee worker safety.

To date, polyvinylidene fluoride (PVdF) is one of the most commonly used electrode binding agents.[7] However, its employment requires harmful solvents [e.g., *N*-methyl-2-pyrrolidone (NMP)] for the slurry preparation. Chasing this greater sustainability, the concept of green binders has been developed according to three different interpretations, that is, considering their (i) processability, (ii) chemical composition, and (iii) natural availability.[8] However, this classification does not consider the sustainability of the entire production cycle that leads to the production of the binder.

In the past years many research groups have systematically adopted Na-carboxymethyl cellulose (CMC) in order to obtain safer and easier-to-handle water-based slurries.[8] CMC, as a series of alternative aqueous binders proposed in literature for electrochemical energy storage, is a fluorine-free compound. In addition, it is cost-effective with respect to PVdF. Thus, its employment could lead to a general cost reduction for EDLCs, which currently, by standardizing the price to the specific energy, are more expensive than LIBs.

Even if CMC has been extensively and successfully utilized, there is a huge interest in finding more alternative green materials. Indeed, like in many other cases in the literature, a

[a] *Dr. A. Scalia,[+] P. Zaccagnini,[+] Prof. M. Armandi, G. Latini, Dr. D. Versaci, V. Lanzio, Prof. A. Lamberti*
Politecnico di Torino, Dipartimento di Scienza Applicata e Tecnologia (DISAT)
Corso Duca Degli Abruzzi, 24, 10129 Torino (Italy)
E-mail: andrea.lamberti@polito.it
[b] *P. Zaccagnini,[+] G. Latini, Prof. A. Lamberti*
Istituto Italiano di Tecnologia
Center for Sustainable Future Technologies
Corso Trento, 21, 10129 Torino (Italy)
[c] *Dr. A. Varzi, Prof. S. Passerini*
Helmholtz Institute Ulm (HIU)
Helmholtzstrasse 11, 89081 Ulm (Germany)
E-mail: alberto.varzi@kit.edu
[d] *Dr. A. Varzi, Prof. S. Passerini*
Karlsruhe Institute of Technology (KIT)
P.O. Box 3640, 76021 Karlsruhe (Germany)
[+] *These authors contributed equally to this work.*

Supporting information for this article is available on the WWW under https://doi.org/10.1002/cssc.202001754

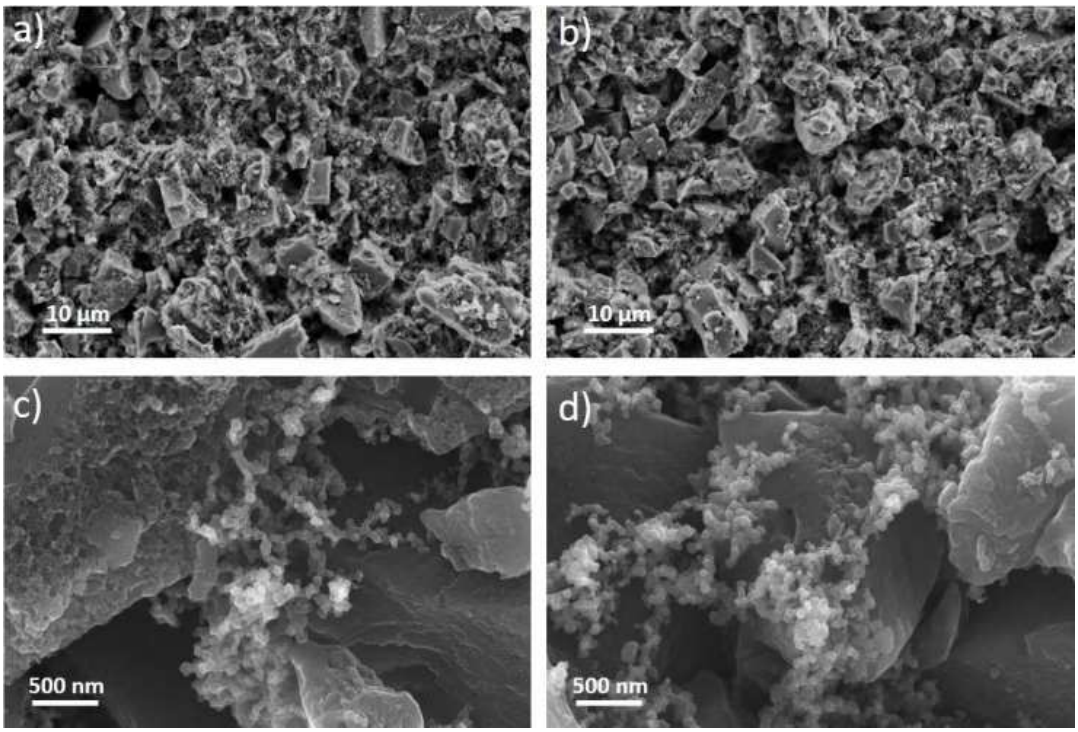

Figure 1. FESEM micrographs showing the morphology at different magnifications of CMC- (a, c) and TRGC-based electrodes (b, d).

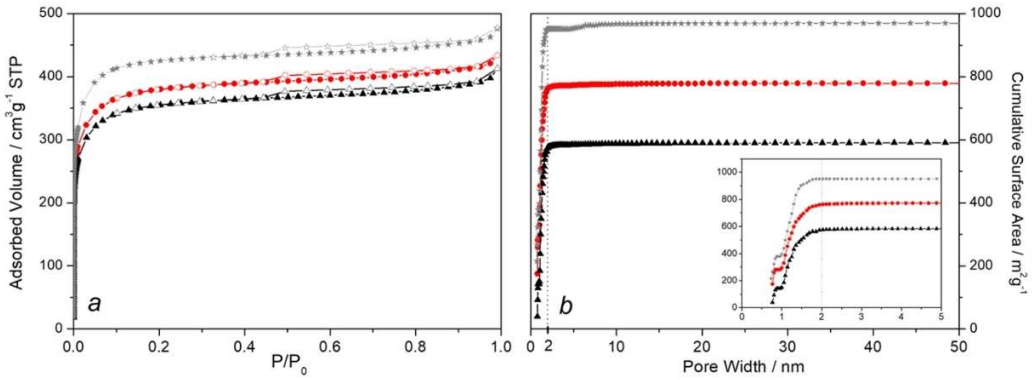

Figure 2. N_2 adsorption/desorption isotherms at 77 K (a) and cumulative surface area curves in the micro–mesopores range (b) of bare AC (stars) and samples prepared using TRGC (circles) or CMC (triangles). Inset of b shows a magnification in the 0–5 nm range.

material is often considered "green" due to its bio-derivation or water solubility, without considering its production process. For example, this is the case for viscose, which is made from natural sources such as wood and agricultural products that are regenerated as cellulose fibers but with a production process that involves highly concentrated sodium hydroxide and carbon sulfide (i.e., corrosive or toxic reagents).[9] Another case, approaching the field of binders for energy storage devices, is represented by chitosan, a bio-derived material that is produced commercially by deacetylation of chitin, exploiting again highly concentrated NaOH solutions.[10] The situation for CMC is similar as it is synthesized by the alkali-catalyzed reaction of cellulose with chloroacetic acid, a hazardous alkylating agent.[11]

Here, we propose for the first time the exploitation of tragacanth (TRGC), a natural gum exudated from some species of gummifer shrub in the Middle Eastern counties, as a truly green binder for supercapacitor electrode fabrication. TRGC has been recently listed as possible candidate for the sustainable fabrication of energy storage devices[8] and was tested in rechargeable batteries with comparable performance to many other bio-derived binders.[12] A comparison with CMC-based slurry is presented, revealing superior electrochemical performance of TRGC, mainly ascribable to a more favorable surface porosity of the electrodes.

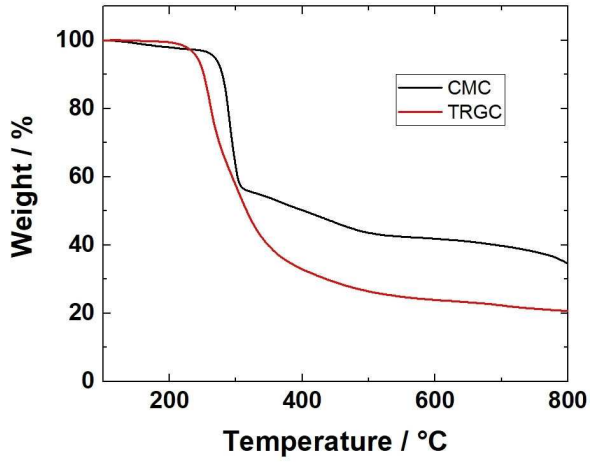

Figure 3. TGA comparison of the two binders.

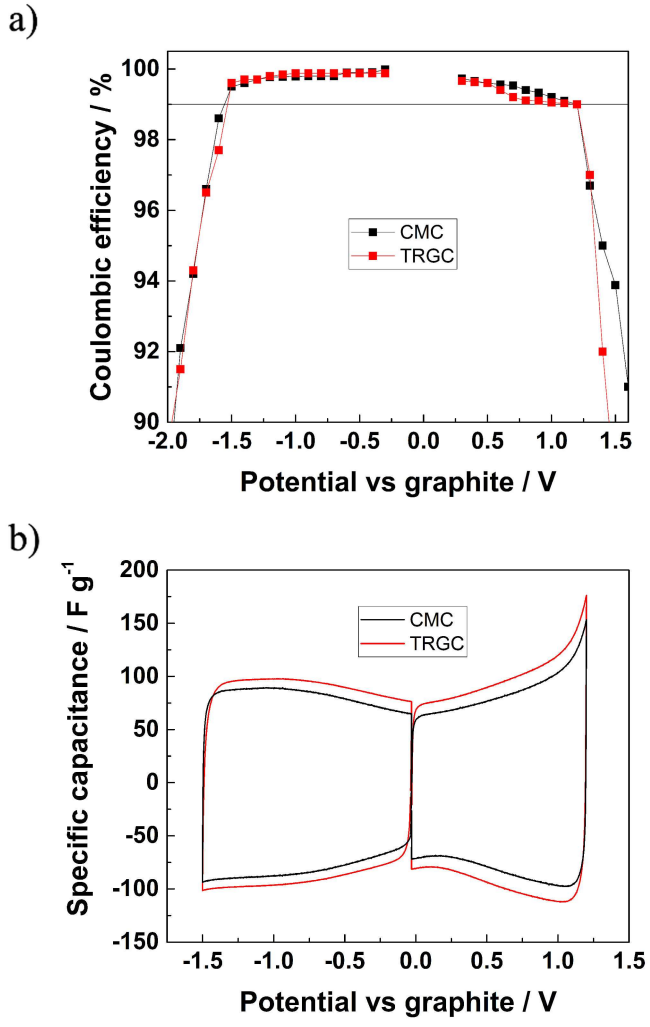

Figure 4. Electrochemical anodic and cathodic stability of electrodes with different binders. a) Coulombic efficiency versus electrode potential recorded at 5 mV s^{-1}; a threshold of 99% was chosen to determine the device voltage. b) Anodic and cathodic voltammograms in specific capacitance representation.

Experimental Section

Electrode preparation

Supercapacitor (SC) composite electrodes were prepared by aqueous processing. Two slurries with composition 85% activated carbon (AC, 1666 $m^2 g^{-1}$ from datasheet), 10% carbon black C65 (CB) and 5% binder (CMC or TRGC), were prepared by stirring in Milli-Q water. Carbon powders were purchased from MTI Corp, binders from Sigma Aldrich. Binders were dissolved first in water (0.1 mL per mg of binding material) by stirring, then CB was added, and the mixtures were let become homogeneous before adding the AC. The mixtures were mixed overnight.

The two slurries were doctor-bladed over Al-foils with wet thickness of 200 μm. The two coatings were let dry for few hours under hood convection, then further dried in an oven at 60 °C. Both coatings were loaded on average with 1.5 mg cm^{-2} active material.

We first studied and compared the anodic and cathodic limits of the electrodes in standard organic electrolyte. Tetraethylammonium tetrafluoroborate (TEA BF_4, 99%) was dissolved in propylene carbonate (PC, anhydrous), both purchased from by Sigma Aldrich, to obtain 1 M solution. Electrodes (18 mm in diameter) were cut and assembled in PAT-CELL for three-electrodes measurement. These cells feature polyethylene (PE) insulation sleeve equipped with carbon pseudo-reference electrode pressed in contact with 160 μm-thick Whatman Glass Fibre GF/A. Thick (18 mm in diameter) self-standing polytetrafluoroethylene (PTFE) electrodes were employed as counter electrodes. Then, we used 15 mm electrodes in Coin Cells 2032, purchased from MTI, separated by GF/A to characterize device performance and 18 mm electrodes in EL-CELLs to study the devices' electrochemical impedance response. All cells were filled with 100 μL of electrolyte and assembled in a glovebox (MBraun) under Ar atmosphere, with 2 mbar overpressure and <1 ppm O_2 and H_2O content.

Physico-chemical characterization

Electron microscopy analysis was performed with a field-emission scanning electron microscope (FESEM Supra 40, Zeiss) equipped with a Si(Li) detector for energy-dispersive X-ray spectroscopy (EDS).

N_2 sorption isotherms were measured at 77 K on electrodes (active material onto current collector) previously outgassed at 200 °C for at least 4 h, in order to remove water and other atmospheric contaminants (Quantachrome Autosorb 1 C instrument). From N_2 isotherms, the Brunauer-Emmett-Teller (BET) specific surface area (SSA) values were measured by multipoint method within the relative pressure range of 0.05–0.15 P/P_0. Micropore areas were calculated from the cumulative surface area curves, as obtained by the non-local density functional theory (NLDFT) method (kernel for nitrogen adsorption at 77 K onto carbon slit-pores). Microporous volume and external surface area (S_{EXT}) were calculated by the *t*-plot statistical thickness method, using a CB thickness equation (fitted thickness range 0.35–0.44 nm).

Static contact angles were studied to verify the wettability of the different samples. Measurements were performed using OCA H200 Dataphysics equipment in ambient conditions. The sessile drop method was implemented employing deionized water droplets and 1 M TEA BF_4 in PC with 1.5 μL volume. Results are mean values of three measurements on different regions of electrode surface.

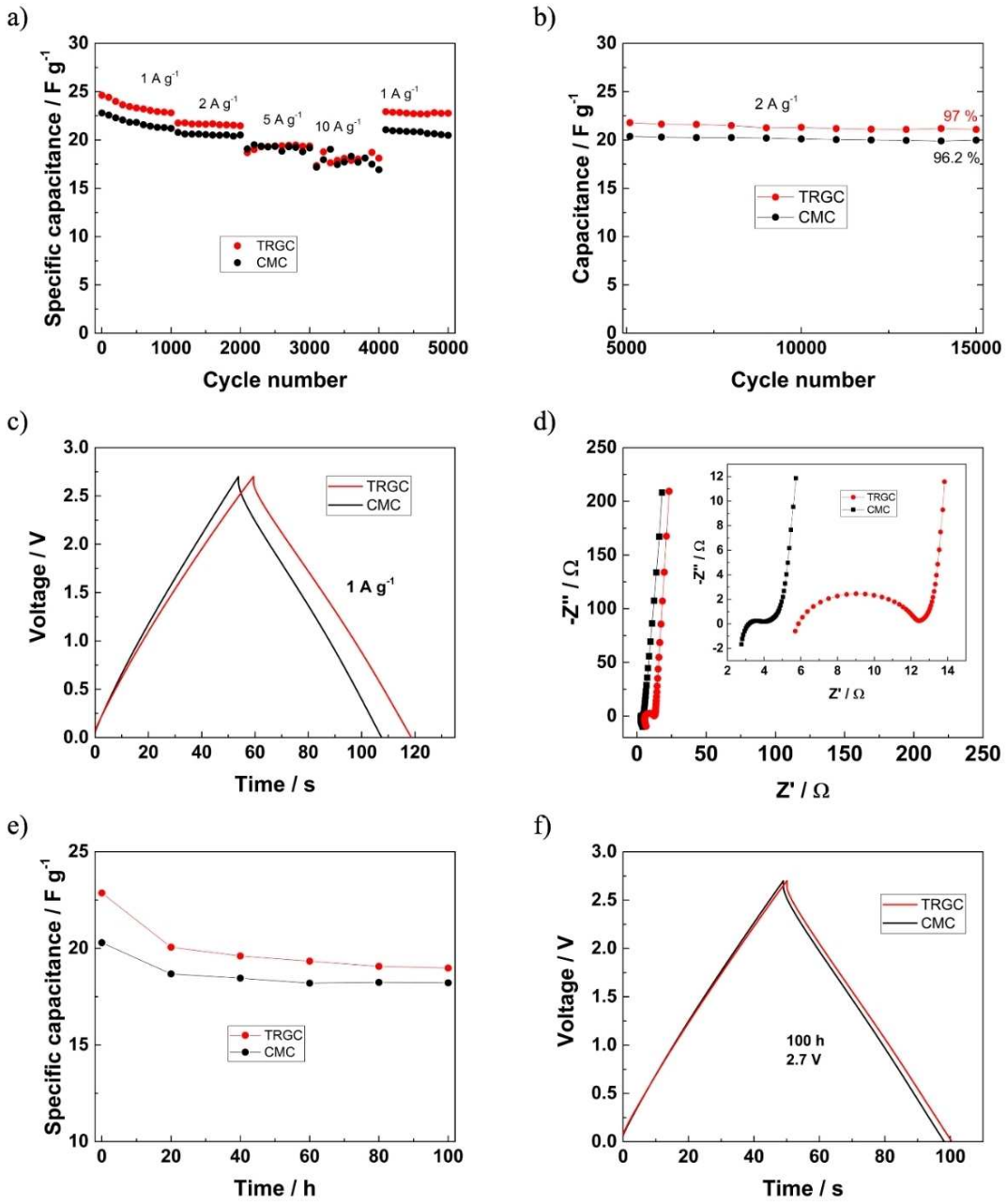

Figure 5. a) Galvanostatic rate capability test; b) galvanostatic cyclability test; c) comparison between the galvanostatic profiles of the two devices; d) Nyquist plot; e) float test results; and f) galvanostatic profiles after 100 h floating.

Thermogravimetric analysis

The thermal stability of both binders was assessed by thermomicrobalance (NETZSCH TG 209 F1 Libra) using an alumina pan as sample holder and approximately 5 mg of sample. The temperature was raised from 30 to 800 °C at a rate of 10 °C min^{-1}. In order to appreciate eventual water content, a 15 min isothermal step at 100 °C was included in the thermal program. The analyses were carried out under nitrogen atmosphere (20 mL min^{-1}).

Electrochemical characterization

Electrochemical impedance spectroscopy (EIS) and cyclic voltammetry (CV) were performed with a Metrohm Autolab equipped with M101 potentiostat/galvanostat and FRA32 M modules. Galvanostatic measurements were performed with Arbin BT2000. Temperature tests were accomplished in a Memmert Oven UN30 with side opening for electrical cables. Electrolyte stability was studied by CV performed at 5 mV s^{-1} while increasing the window stepwise after every 10 cycles. These tests were run in three-electrode configuration. From these measurements we obtained the electrode mass ratio in order to exploit the full electrolyte stability window. Then, we moved to device characterization. We performed at first CVs at

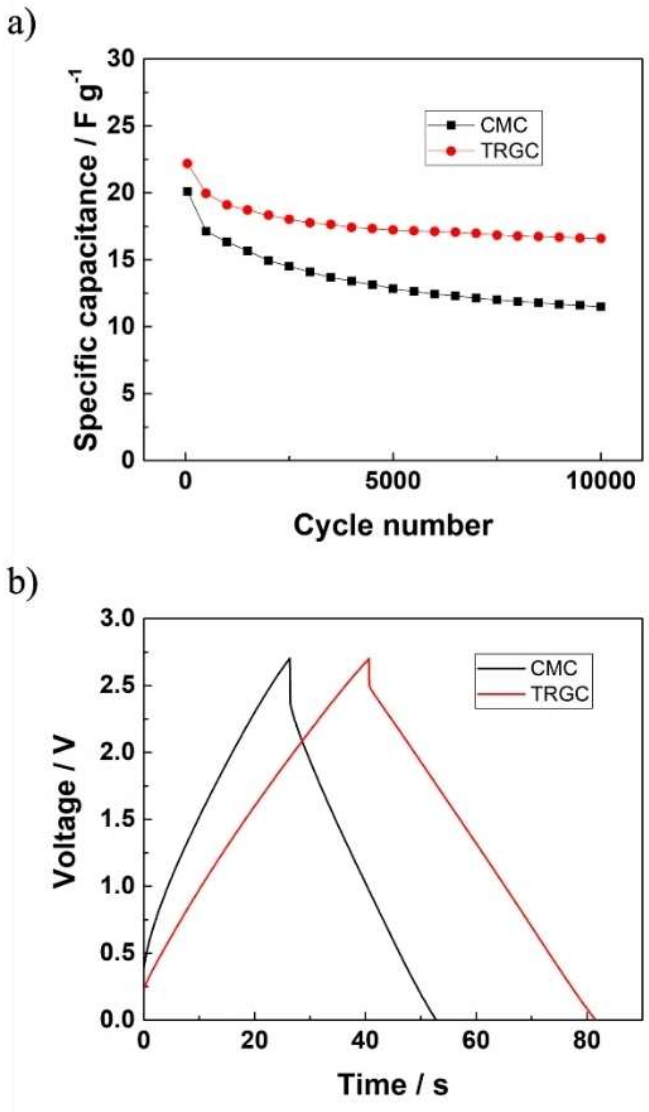

Figure 6. Temperature test cycling carried out at 70 °C. a) Capacitance retention and b) voltage profiles in the10000th cycle at 1 A g^{-1}.

several scan rates and EIS with $V_p = 5$ mV and frequencies ranging from 1 MHz down to 10 mHz acquiring five points per decade. Galvanostatic measurements were run following an initial protocol aimed to evaluate the device rate capability, and then the cells were left cycling for 50000 cycles. Floating tests were also performed in order to evaluate device endurance under constant high-voltage conditions.

Capacitances were derived from the energy, which was computed according to Equation (1):

$$E = \int V(t)I(t)\mathrm{d}t \quad (1)$$

and using Equations (2) and (3):

$$E = \frac{1}{2}\frac{Q^2}{C} \quad (2)$$

$$Q = \int I(t)\mathrm{d}t \quad (3)$$

The power was calculated by applying Equation (4):

$$P = \frac{E}{\Delta t} \quad (4)$$

where Δt represents the discharge time, since all quantities were computed in discharge.

Results and Discussion

The chemical structures of CMC and TRGC are reported in Figure S1. Both TGRC and CMC are biopolymers that shares the same cellulose backbone. They differ in the functional group linked to the main polymer chain. In TGRC, glucose rings are linked to the cellulose chain, whereas in CMC, alcoholic hydrogen can be substituted with sodium methyl carboxylate ($-CH_2COO^-\ Na^+$).

In order to evaluate the effect of the different binders on the quality of electrodes we prepared some samples to be characterize by SEM. Figure 1 collects different magnification of the SEM micrographs taken on the CMC and TRGC-based carbon electrodes. AC porous macroparticles and nanometric CB particles are clearly recognized, whereas it is impossible to identify the morphologic contribution coming from the binders. However, it is possible to state that no particular effects are introduced by the substitution of CMC with TRGC in terms of particle spatial distribution, film uniformity, cohesion, and adhesion.

The effect of the adopted binder on the porous properties of the carbon material was investigated by means of N_2 adsorption measurements at 77 K, the results of which are gathered in Table 1. Both samples showed the same type I isotherm of the bare AC (Figure 2a), with very limited hysteresis

Table 1. Surface parameters as evaluated by the data shown in Figure 2.

Material	SSA_{BET} [$m^2 g^{-1}$]	Micropore area[a] [$m^2 g^{-1}$]	V_{TOT}[b] [$cm^3 g^{-1}$]	V_{micro}[c] [$cm^3 g^{-1}$]	V_{micro}[d] [$cm^3 g^{-1}$]	S_{EXT}[d] [$m^2 g^{-1}$]
AC	1590	963	0.74	0.64	0.60	261
TRGC	1424	765	0,65	0.54	0.51	256
CMC	1330	576	0,60	0.50	0.46	243

[a] According to NLDFT, measured from cumulative surface area curves at 2 nm. [b] Measured from isotherms at $P/P_0 = 0.95$. [c] According to NLDFT, measured from cumulative pore volume curves at 2 nm. [d] According to the *t*-plot method.

loop (type H4), as commonly observed with porous carbons.[13] The sample prepared using binder CMC showed lower SSA_{BET} and total pore volume, suggesting a more pronounced pore blocking effect due to the binder. Although widely used in literature, the BET method is not strictly suited to the study of microporous materials, especially when comparing materials with different microporosity.[13c]

We therefore used the NLDFT method to measure the microporous surface area and volume of the samples. Interestingly, the analysis of the obtained cumulative surface area curves clearly shows that the microporous surface area (i.e., area of pores with width smaller than 2 nm) of the sample prepared with CMC is approximately 25% lower than that of sample prepared with TRGC, clearly evidencing the importance of the chosen binder. Accordingly, the *t*-plot analysis showed that the decrease in surface area and porous volume is mainly due to the loss of microporosity, with limited decrease in the S_{EXT}. The resultant microporous volumes were also in good agreement with those obtained by NLDFT method.

The thermal stability of TRGC was evaluated by thermogravimetric analysis (TGA; Figure 3 reports thermograms of dried samples). The TGA curve of CMC showed a two-stage weight loss at 290 and 450 °C. The initial weight loss of about 39% was due to the decomposition of the cellulose carboxylate functional group in form of CO_2 and water. The second weight loss of 20% was due to the degradation and carbonization of the polymer backbone.[14] The thermogram of TRGC showed two main degradation stages at 258 and 306 °C, as evaluated by the weight loss derivative curve. The two steps superimpose, and the weight loss is about 76%. The whole degradation process could be ascribed to the initial decomposition of the labile pendant functional groups of the TRGC building blocks and the following polymer backbone decomposition and carbonization.[15]

Finally, the wettability of the electrodes was investigated by means of contact angle measurements. The results are reported in Figure S2. As can be observed, TRGC showed a lower contact angle than CMC when water was used, thus being more hydrophilic. Concerning the electrolyte solution (1 M TEA BF_4 in PC), both the electrodes exhibit very low contact angles, with a slightly lower value for CMC-based electrodes. As a visible feedback, we observed rapid electrode wetting for both the test liquid selected, as observed with the electrolytic solution during the assembling procedures.

Next, electrochemical measurements were performed in order to assess the behavior of the different materials. A first set of measurements was conducted in three-electrode configuration in PAT cells with carbon core reference, provided by EL-Cell test equipment. The use of the latter material as a pseudo-reference has been proved to be of practical use in the work of Ruch et al., especially with the standard electrolyte TEA BF_4 1 M in PC.[16] Bulky carbon electrodes were used as counter electrodes (CE) in order not to limit the response of the working electrode (WE). The potential of the WE was spanned at 5 mV s^{-1} from the open-circuit voltage (OCV) to different anodic and cathodic cut-off potentials, and the coulombic efficiency was evaluated (see Figure 4). Figure 4a clearly shows that the novel binder does not alter the voltage window of the electrolyte. In contrast, as reported in Figure 4b, it markedly affects the electrode capacitance, confirming the lower impact of TRGC on the SSA compared to CMC (see previously discussed surface area analysis).

Concerning the voltage window, it is evident from Figure 4a that the anodic limit is almost +1.2 V, whereas the cathodic one is approximately −1.5 V. We then applied the charge-balance equation $m_-Q_- = m_+Q_+$ in order to find the proper mass ratio between the anode and cathode so to exploit the full electrolyte voltage window of 2.7 V.

Properly balanced EDLCs were electrochemically characterized in 2032-coin cells. Concerning galvanostatic charge and discharge (GCD) results, we first ran a rate capability test by changing the current density every 1000 cycles (Figure 5). We started from 1 up to 10 A g^{-1} and then let the devices cycle at 1 A g^{-1} for 10000 cycles. In both cases devices demonstrated a good rate capability (less than 25% capacitance loss at 10 A g^{-1}) with a better result for the CMC-based devices. However, it can be appreciated that by decreasing the current rate the specific capacitance increases again for the TRGC-based device.

Both devices showed a good capacity retention after 10000 at 1 A g^{-1}, as reported in Figure 5b. In Figure 5c we display the GCD profiles comparison at 1 A g^{-1}. It was found that the CMC-based electrode is more conductive as can be appreciated from the AC impedance results shown in Figure 5d. The semicircle present in the TRGC device could be attributed to a hindered transport in the electrode caused by the binder itself.[17] These results reflect what was obtained during the rate capability test: the slightly higher resistive behavior of the TRGC device does not allow higher capacity retention compared to CMC. Our conclusion is that TRGC does not substantially alter the capacitance of the electrodes. Indeed, it seems to affect the porosimetric properties of the AC less than CMC. However, it does partially hinder the electrical transport, which can explain the inferior rate capability.

In order to evaluate the long-term stability of the new binder, we ran a float test for 100 h. The results are depicted in Figure 5e,f. Device capacitances were record every 20 h after being kept at device maximum-rated voltage. It can be observed that both devices experience a capacitance loss, which in the case of TRGC is 17%, whereas in the case of CMC it is slightly lower (12.5%). However, at the end of the test TRGC devices did show higher specific capacitance. At the end of the test, after 100 h, the overall cells characteristics were not significantly altered as can be observed in Figure 5f.

Finally, temperature tests were run in order to evaluate the temperature stability of the electrodes. Devices were let cycle at 1 A g^{-1} at 70 °C at rated voltage window. As can be observed from Figure 6, TRGC electrodes present a better temperature stability.

Conclusions

In conclusion, in this paper we proposed the exploitation of tragacanth gum (TRGC) as green aqueous binder for super-

capacitor electrode fabrication. Na-carboxymethyl cellulose (CMC)-based electrodes were fabricated using the same active material, resulting in a higher performance of TRGC over CMC. We attributed this improvement to the higher available surface area of the TRGC-based electrodes, probably affected by the higher pore occlusion induced by CMC. Indeed, the capacitive properties of the electrodes were not altered. Devices based on gum showed a specific capacitance of 23 $F g^{-1}$, whereas cellulose-based ones showed 21 $F g^{-1}$ in standard organic electrolyte tetraethylammonium tetrafluoroborate with concentration of 1 M in propylene carbonate. Even though we observed a slight loss in rate capability, devices with the novel binder showed a remarkable thermal stability at elevated temperatures.

Acknowledgements

The authors would like to acknowledge Ms. Gaia Di Martino (Polytechnic of Turin) and Dr. Sergio Bocchini (Italian Institute of Technology) for the useful discussion on the sustainability of some polymers' production processes. A.V. and S.P. thank the Helmholtz Association for the financial support Open access funding enabled and organized by Projekt DEAL.

Conflict of Interest

The authors declare no conflict of interest.

Keywords: aqueous processing · green binder · high temperature · supercapacitors · tragacanth

[1] a) K. H. An, W. S. Kim, Y. S. Park, J. M. Moon, D. J. Bae, S. C. Lim, Y. S. Lee, Y. H. Lee, *Adv. Funct. Mater.* **2001**, *11*, 387–392; b) A. González, E. Goikolea, J. A. Barrena, R. Mysyk, *Renewable Sustainable Energy Rev.* **2016**, *58*, 1189–1206.
[2] a) M. Conte, *Fuel Cells* **2010**, *10*, 806–818; b) A. Rufer, D. Hotellier, P. Barrade, *IEEE Trans. Power Delivery* **2004**, *19*, 629–636.
[3] a) C. Zhong, Y. Deng, W. Hu, J. Qiao, L. Zhang, J. Zhang, *Chem. Soc. Rev.* **2015**, *44*, 7484–7539; b) A. Scalia, A. Varzi, A. Moretti, P. Ruschhaupt, A. Lamberti, E. Tresso, S. Passerini, *ChemElectroChem* **2019**, *6*, 552–557.
[4] P. Simon, Y. Gogotsi, B. Dunn, *Science* **2014**, *343*, 1210–1211.
[5] a) C. Yin, H. Wu, F. Locment, M. Sechilariu, *Energy Convers. Manage.* **2017**, *132*, 14–27; b) M. E. Glavin, P. K. W. Chan, S. Armstrong, W. G. Hurley, *13th International Power Electronics and Motion Control Conference, EPE-PEMC 2008*, **2008**, pp. 1688–1695; c) A. Scalia, A. Varzi, A. Lamberti, E. Tresso, S. Jeong, T. Jacob, S. Passerini, *Sustainable Energy Fuels* **2018**, *2*, 968–977; d) A. Scalia, F. Bella, A. Lamberti, S. Bianco, C. Gerbaldi, E. Tresso, C. F. Pirri, *J. Power Sources* **2017**, *359*, 311–321; e) A. Scalia, F. Bella, A. Lamberti, C. Gerbaldi, E. Tresso, *Energy* **2019**, *166*, 789–795.
[6] a) M. Raja, B. Sadhasivam, R. Janraj Naik, R. Dhamodharan, K. Ramanujam, *Sustainable Energy Fuels* **2019**, *3*, 760–773; b) S. S. Jeong, N. Böckenfeld, A. Balducci, M. Winter, S. Passerini, *J. Power Sources* **2012**, *199*, 331–335; c) H. H. Rana, J. H. Park, G. S. Gund, H. S. Park, *Energy Storage Mater.* **2020**, *25*, 70–75; d) S. K. Park, H. Lee, M. S. Choi, D. H. Suh, P. Nakhanivej, H. S. Park, *Energy Storage Mater.* **2018**, *12*, 331–340; e) J. H. Park, H. H. Rana, J. Y. Lee, H. S. Park, *J. Mater. Chem. A* **2019**, *7*, 16962–16968; f) P. Ruschhaupt, A. Varzi, S. Passerini, *ChemSusChem* **2020**, *13*, 763–770.
[7] a) O. Chernysh, V. Khomenko, I. Makyeyeva, V. Barsukov, *Materials Today: Proceedings, Vol. 6*, **2019**, pp. 42–47; b) Z. Zhu, S. Tang, J. Yuan, X. Qin, Y. Deng, R. Qu, G. M. Haarberg, *Int. J. Electrochem. Sci.* **2016**, *11*, 8270–8279.
[8] D. Bresser, D. Buchholz, A. Moretti, A. Varzi, S. Passerini, *Energy Environ. Sci.* **2018**, *11*, 3096–3127.
[9] H. Sixta, H. Harms, S. Dapia, J. C. Parajo, J. Puls, B. Saake, H. P. Fink, T. Röder, *Cellulose* **2004**, *11*, 73–83.
[10] I. Muñoz, C. Rodríguez, D. Gillet, B. M. Moerschbacher, *Int. J. Life Cycle Assess.* **2018**, *23*, 1151–1160.
[11] T. Shui, S. Feng, G. Chen, A. Li, Z. Yuan, H. Shui, T. Kuboki, C. Xu, *Biomass Bioenergy* **2017**, *105*, 51–58.
[12] D. Versaci, R. Nasi, U. Zubair, J. Amici, M. Sgroi, M. A. Dumitrescu, C. Francia, S. Bodoardo, N. Penazzi, *J. Solid State Electrochem.* **2017**, *21*, 3429–3435.
[13] a) L. Osmieri, R. Escudero-Cid, M. Armandi, A. H. A. Monteverde Videla, J. L. García Fierro, P. Ocón, S. Specchia, *Appl. Catal. B* **2017**, *205*, 637–653; b) M. Armandi, B. Bonelli, F. Geobaldo, E. Garrone, *Microporous Mesoporous Mater.* **2010**, *132*, 414–420; c) M. Thommes, K. Kaneko, A. V. Neimark, J. P. Olivier, F. Rodriguez-Reinoso, J. Rouquerol, K. S. W. Sing, *Pure Appl. Chem.* **2015**, *87*, 1051–1069.
[14] a) M. J. Zohuriaan, F. Shokrolahi, *Polym. Test.* **2004**, *23*, 575–579; b) D. de Britto, O. B. G. Assis, *Thermochim. Acta* **2009**, *494*, 115–122; c) R. J. Evans, T. A. Milne, *Energy Fuels* **1987**, *1*, 123–137.
[15] D. Dollimore, R. Karimian, *Thermochim. Acta* **1981**, *51*, 353–361.
[16] P. W. Ruch, D. Cericola, M. Hahn, R. Kötz, A. Wokaun, *J. Electroanal. Chem.* **2009**, *636*, 128–131.
[17] a) Y. R. Nian, H. Teng, *J. Electroanal. Chem.* **2003**, *540*, 119–127; b) S. Dsoke, X. Tian, C. Täubert, S. Schlüter, M. Wohlfahrt-Mehrens, *J. Power Sources* **2013**, *238*, 422–429.

Manuscript received: July 22, 2020
Revised manuscript received: October 20, 2020
Accepted manuscript online: October 23, 2020
Version of record online: November 17, 2020